36th International North Sea Flow Measurement Workshop
22-24 October 2018

Technical Paper

Laboratory & Field Test Results for an Adjustable DP Cone Meter

Gavin Munro, GM Flow Measurement Services Ltd
Victor Gawski, GM Flow Measurement Services Ltd

1 INTRODUCTION

This paper describes the development, laboratory and field testing of an adjustable, differential pressure cone flow meter, for accurate gas measurement. Adjustability is achieved using an internal sliding sleeve, which moves in relation to a fixed position cone. The 4" model most recently tested, had two sleeve positions (or operating flow ranges), having a β ratio of 0.7 and 0.45 respectively. A close-coupled flow computer, with integral multi-variable transmitter and Resistance Temperature Device (RTD), monitors the differential pressure, flowing pressure and flowing temperature.

The flow computer uses these parameters and dry gas calibration data to compute the gas density, compressibility, expansibilty, mass, then mass and volume flow rate, according to the user's choice of applicable standards. It does this once per second. If any parameters move outside pre-set limits, the flow computer switches the flow range by controling an air driven motor, to move the sleeve to the desired meter operating pressure range. As the sleeve moves the flow computer monitors its movement, switching the calculations between the 0.7 or 0.45 β ratio and calibration criteria accordingly.

A 6" prototype meter with 0.75 and 0.5 B ratio ranges, was first calibrated at NEL, then field tested on two wells in the North Sea during 2016, proving the concept. The meter design has since been enhanced and a production model was tested with dry and wet gas at NEL during September 2018. The objective was to validate and characterise the meter in terms of assessing its similarities and differences to established theory and published performance characteristics for conventional cone meters.

Flow laboratory test results and initial analysis and findings for the adjustable cone meter are presented. Further characterisation of the meter which was tested in the flow laboratory is ongoing, via live field testing in Oman. Additional flow laboratory validation and characterisation is planned for early 2019.

2 PROTOTYPE METER DESIGN & 2016 NORTH SEA FIELD TRIAL

2.1 Background

A conventional differential pressure cone flow meter provides some advantages over an orifice plate for gas meaurement, particularly in portable test separator applications. It is known that the dual chamber orifice fittings which are commonly used, can be subjected to less than ideal installation, maintenance and use practices.

Examples, include the use of orifice plates which are at the limits of, or even beyond, the β ratios recommended by ISO-5167-2 [1]. It is not uncommon for a

0.5″ orifice plate to be used in a 5.761 inch internal diameter flowline. (β ratio = 0.086). To maintain as small a footprint as possible, the space in which the orifice plate meters are installed is also generally very restricted. In virtually all cases, three-out-of plane, 90-Degree elbows are located at a distance within eight to ten times the pipe diameter (8-10D) upstream of the meter. The dimensions which are commonly used, pertain to column 5 of table 3 of ISO-5167-2 [1]. This provides a recommended minimum of 19D upstream for small β ratios and 44D for larger β ratios, which is seldom achieved in the field. Typical set-up of portable separator gas flowlines are shown in Fig. 1 and 2

Most installations try to overcome this situation by the use of a 19-tube bundle flow straightener, generally located around 5-6D upstream of the orifice plate. ISO-5167-[1] recommends 13.5 to 14.5D in column 4 of table 4, so it is likely that in a majority of occasions, increased incertainty is being introduced, especially at low β ratios. Alternatively, some users have utilised two parallel flow-lines, containing meters, valves and instruments, adding to the capital cost, road (or crane) weight and to maintenance costs.

Fig. 1 – End Cap Gas Line

Fig. 2 – Top Exit Gas Line

ISO-5167 Part 5 [2] states that standard cone meters can be installed with only 6D upstream and 3D downstream, therefore, in space-restricted test separator applications, cone meters should provide less uncertainty than orifice plates. See Fig. 3 for installation requirements of DP cones with 6D upstream compared to orifice plates with 19D and 44 D upstream straight length requirements.

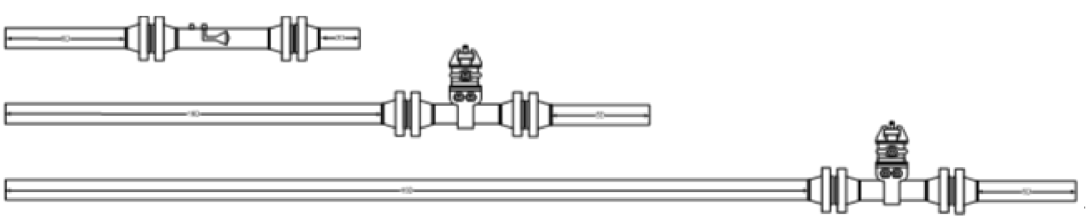

Fig. 3 – DP Cone and Orifice Plate Meters – Upstream Pipe Length Requirements.

Some users express safety concerns relating to orifice plate changing operations, regarding exposure of their personnel to flammable and possibly poisonous H2S gas.

During a typical well test on a new well, the flow rates are increased or decreased to assess reservoir size and performance. Experienced operators have to perform the 30 minute plate changing process every time the flow rate changes significantly, resulting in five to eight gas release events during the testing of a typical exploration well.

Field operational constraints and functional concerns prompted development of the concept of an 'adjustable' cone flow meter. Referencing conventional differential pressure (DP) cone meters as the base technology, an adjustable cylindrical sleeve was located within the bore of the meter housing.

The sliding sleeve interacts with the stationary cone, in its simplest form it effectively produces two cone meter settings within a single meter body. This adjustable cone meter has enhanced turndown ratio range and offers reduced installation space and weight benefits, relative to achieving an enhanced turndown ratio range by operating two different sized conventional cone meters in parallel.

Some users have raised concerns regarding cones being dislodged and diplaced downstream during meter use. Suspecting that such occurrences were the result of the cones reaching a natural frequency, then failing due to fatigue, Finite Element Analysis and Computational Fluid Dynamics analysis were used to determine the behaviour of various cone and stem designs under an extensive range of flow conditions and bracing styles.

2.2 Design Details

The meter sleeve incorporates polymer seals which interact with the bore of the meter housing, creating a pressure seal. Various designs exist to provide movement of the sliding sleeve, including pneumatic and hydraulic. The meter which was tested employed an air motor, pressure sealed gearbox and rack and pinion mechanism.

The bore of the sliding sleeve has a variable profile. It incorporates tapered entrance and exit throats and areas between the thoats which are of specific geometries, both cylindrical and tapered.

The annular restriction produced between the sleeve and cone is governed by the position of the sleeve relative to the cone, by the geometry of the sleeve bore and of the cone, in the vicinity of the cone's largest diameter.

In the low β ratio range, the sleeve covers the cone at the cone outside diameter (β edge) [2] producing the smaller β ratio. The small β ratio is calculated between the cone outside diameter and the sleeve bore diameter. In the high β range, the sleeve moves downstream of the cone, leaving the cone outside diameter uncovered. The β ratio is then calculated between the housing bore diameter and the cone outside diameter. The large and small β ratios are selected to provide an overlap between their separate operating envelopes. This produces one continuous and larger operating envelope, from the partial merging of the two individual envelopes.

For the adjustable meter, see Fig 4. and Eq. 1 and Eq. 2 for details of the two β calculations. These take the same form as equation (2) from ISO 5167-5 [2]

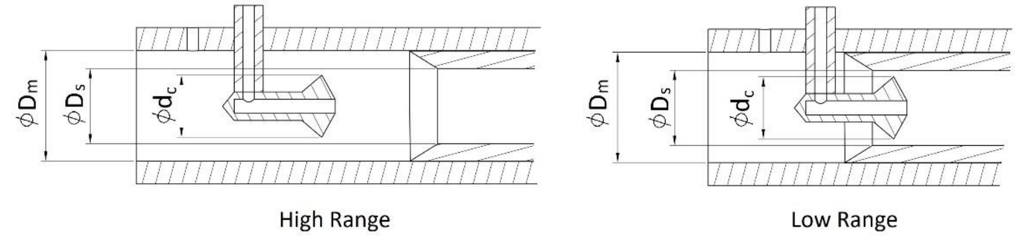

Fig. 4 – Adjustable Cone Meter - Calculaton of the B Ratios

$$\beta_{low} = \sqrt{1 - \frac{d_c^2}{D_s^2}} \quad (1)$$

$$\beta_{high} = \sqrt{1 - \frac{d_c^2}{D_m^2}} \quad (2)$$

(see parameter definition list section 5)

For comparison, Fig 5 and Eq. 3 show a standard cone and the β calculation from IS0-5167-5 [2].

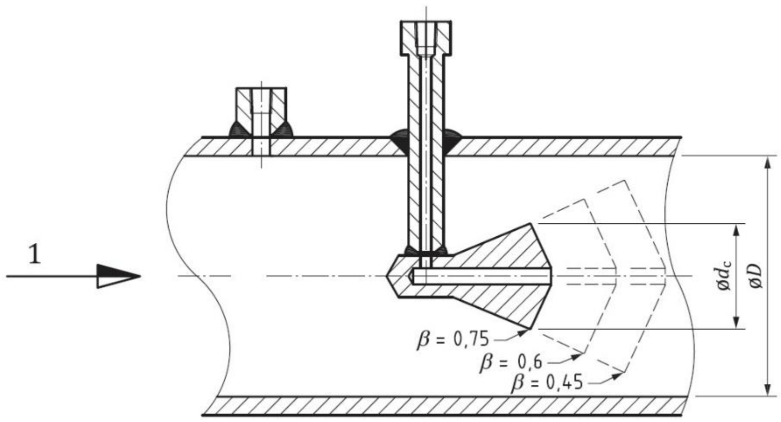

Fig. 5 – Standard Cone Meter showing different values of β [2]

$$\beta = \sqrt{1 - \frac{d_c^2}{D^2}} \quad (3)$$

Standard cone meter β calculation [2]

As with standard cone meters, the mass flow rate for the adjustable cone was calculated using equations 4 and 5, which are identical to ISO-5167-2 [1] equations (1) and (2)

$$q_m = \frac{C}{\sqrt{1-\beta^4}}\,\varepsilon\,\frac{\pi}{4}\,(D\beta)^2\sqrt{2\Delta p \rho_1} \quad (4)$$

Where

$$\epsilon = 1 - (0.649 + 0.696\,\beta^4)\frac{\Delta p}{k p_1} \quad (5)$$

as described by Steward et al. [5]

And Volume flow rate calculated using equation 6

$$q_v = \frac{q_m}{\rho} \quad (6)$$

However, the adjustable cone meter has two different β ratios, for the high and low meter operating ranges, having corresponding coefficients of discharge. See section 3.2 for calibration method.

2.2.1 Cone Stem

The cone stem design was refined and strengthened, the cone being made both lighter and braced depending on size. Vibration analysis was performed with various cone, stem and support designs. Typical resonant frequency analysis is shown in Table 1. The resulting cone design will not reach its first natural frequency during operation. The design of the cone, meter housing and sleeve bores have been optimised, such that they have very low susceptibility to erosion damage (see Fig. 6 and Fig 7).

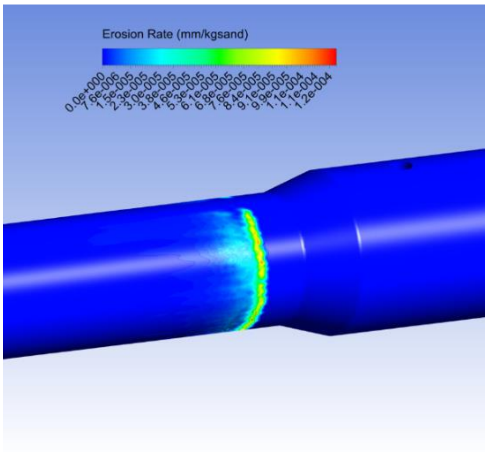

Fig.6 Fluid Erosion Analysis

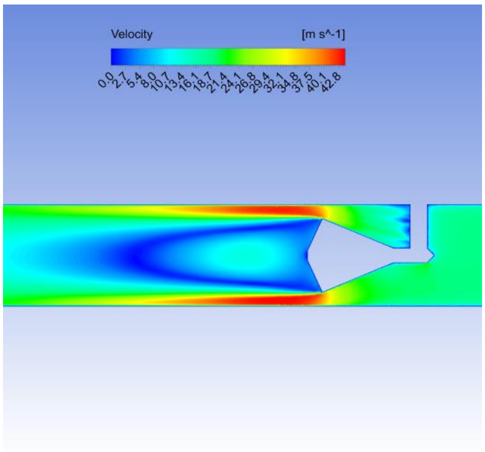

Fig.7 Velocity Analysis

Table 1 - Cone Vibration Analysis

Mode	Natural Frequency (Hz)	Vibration Axis & Direction
1	342.9	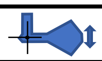
2	368.6	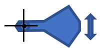
3	1268.4	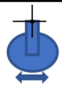

The prototype meter was manually controlled, using a 3-way ball valve to divert air to a reversible air motor. The motor was connected to a reducing gearbox and a rack and pinion mechanism (Fig. 8) which allowed the sleeve to be moved in opposing directions. The reducing gears were self-locking, preventing possible sleeve movement, which could result from the action of differential pressure on the sleeve cross-sectional area.

Sleeve movement and position, was detected using a pointer attached to the end of the pinion drive shaft, indicating the meter 'high' and 'low' flow operating range (see Fig. 9).

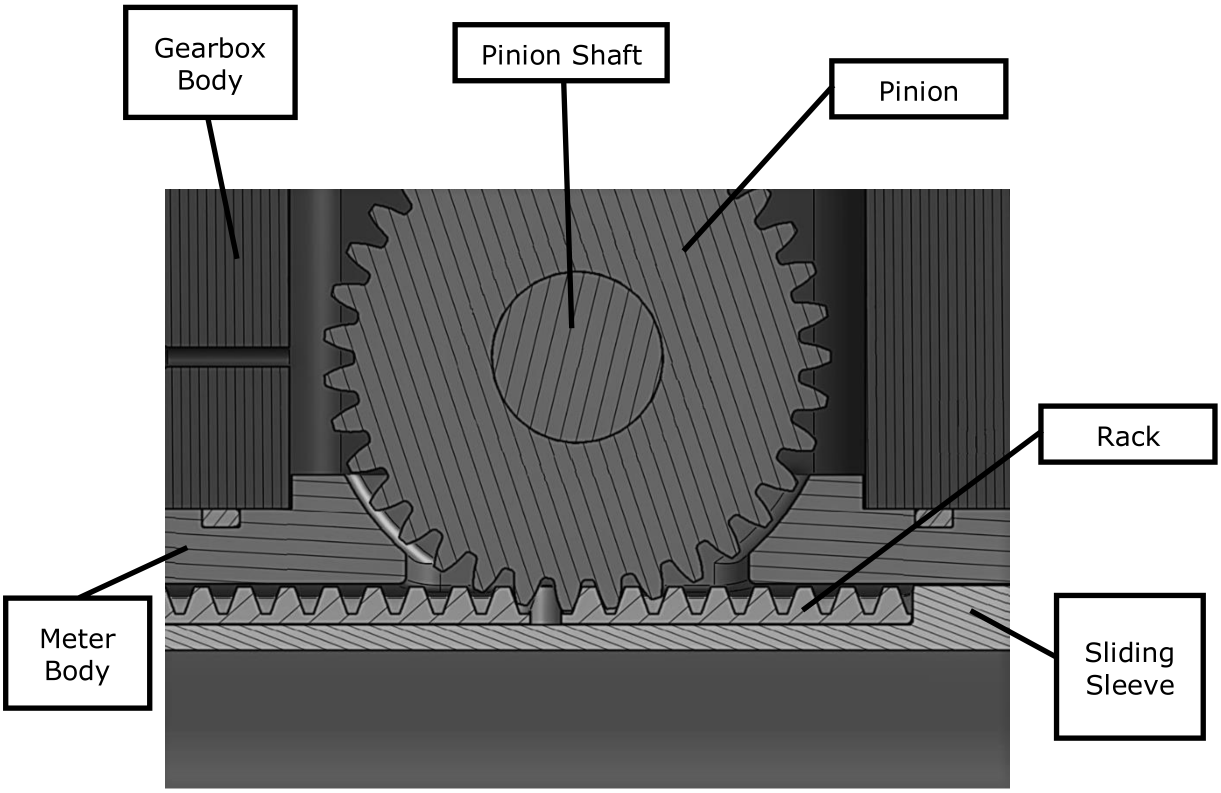

Fig. 8 Rack & Pinion Mechanism

Fig. 9 Early Design Sleeve Position Indicator

The meter pressure tappings were located at the top of the meter housing relative to the meter’s horizontal operating orientation. The high pressure tapping was sized and positioned upstream of the cone according to ISO-5167 part 5 [2]. The low pressure tapping was positioned within the cone, the diameter of the low pressure tapping was designed according to ISO-5167 part 5 [2].

The parameters used for determining whether to use high or low flow range were~~;~~ differential pressure and flowing velocity. Reynolds number and flow rate were also monitored and recorded. At this stage, the sleeve position was manually changed, with all decisions being made by technicians, overseeing the operation.

2.3 Laboratory Calibration

The 6” meter was dry calibrated at NEL Flow Laboratory, East Kilbride, UK, at 10 and 62 Bar(g) with dry Nitrogen gas and a series of coefficients of discharge and corresponding Reynolds numbers were obtained using equation (7) [6]. Calibration data for the 0.75 and 0.5 β range are shown in Fig. 10 and 11. The data labeled “Flow Computer Data” is the Coefficient of Discharge and Reynolds Number data which was entered into the flow computer for the field trials.

$$C = \frac{m\sqrt{1-\beta^4}}{\epsilon A_a\sqrt{2\rho_1 \Delta p}} \qquad (7)$$

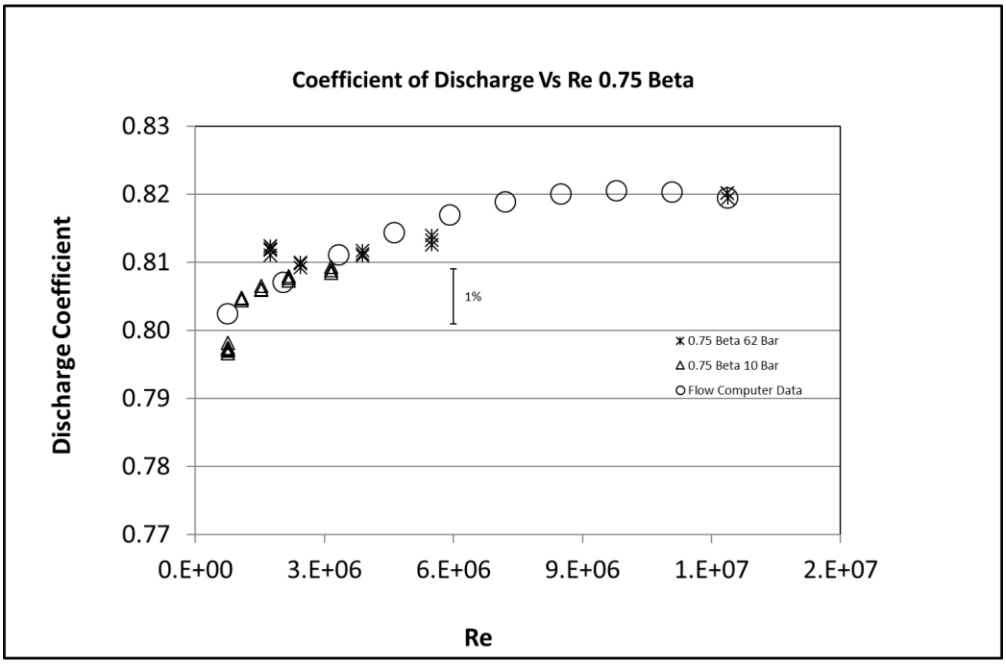

Fig. 10 Dry N2 Calibration Results for the 0.75 β Ratio Range

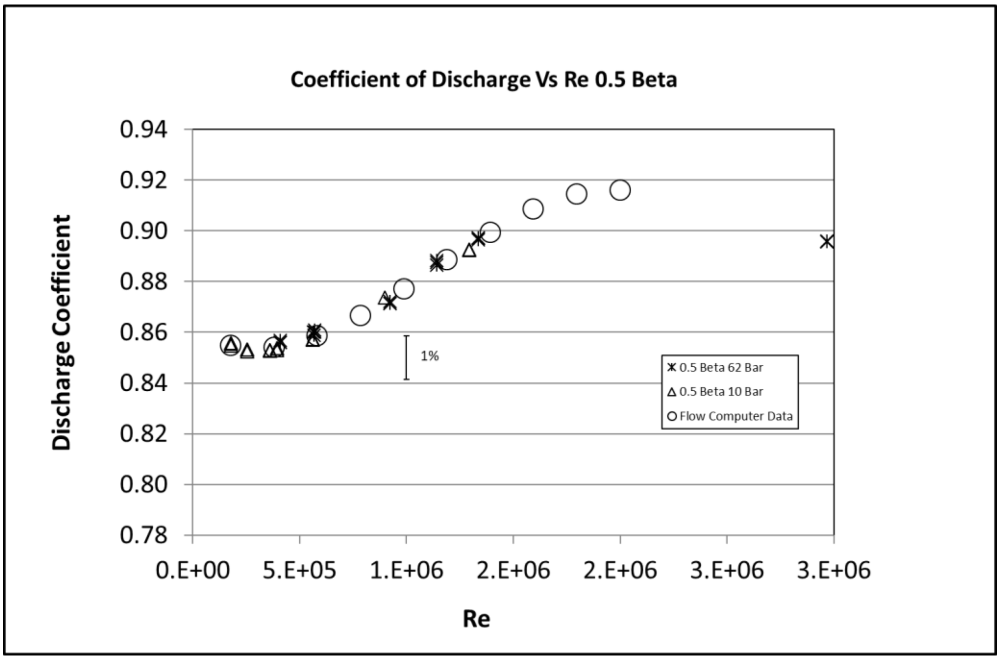

Fig. 11 Dry N2 Calibration Results for the 0.5 β Ratio Range

2.4 Field Testing Objectives

Meter Size 6″ 600 lb RF with 0.75 and 0.5 β ratio ranges

The first protototype 6″ internal diameter meter was calibrated at NEL during November 2015 (6″ meter designation relates to the associated pipe size). It was then field tested offshore on two wells in the North Sea, during the summer of 2016. The objective was to make performance comparison with an existing orifice plate and to prove the functionality of the sleeve moving mechanism under field conditions, during well testing operations. (Fig.12).

2.4.1 Field Test 1

The meter was installed downstream from a portable test separator, fitted with a 6″ dual chamber orifice fitting. Due to operational constraints the meter had to be assembled into the flowline, downstream of the separator Pressure Control Valve (PCV), while the orifice plate was installed upstream of the PCV. It was therefore expected that flowing pressure and DP in the cone meter would be very low, since no other restrictions, other than line pipe, existed between the meter and the flare.

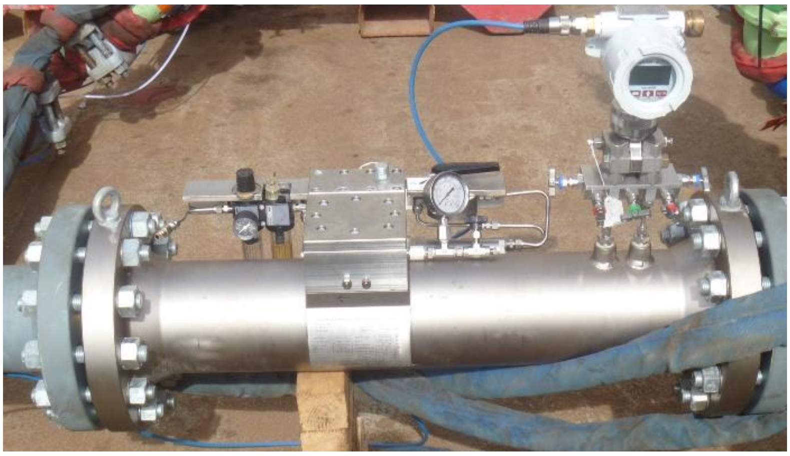

Fig. 12 – 6″ Prototype Meter Offshore North Sea in 2016

The end user calculated that at his expected flow rates, around 10-20 PSIG (0.69 – 1.34 Bar) of pressure would be observed at the cone meter. In the 0.75 β ratio position, it would therefore produce between 10 and 20 Inches of H2O differential pressure (25-50 mBar). In this case, it was decided to utilise a flow computer with 100 psia and 30″ H2O range in order to try to measure the flow rate successfully.

During the trial the gas flowed at only 15% of that expected, so the meter was adjusted to the 0.5 β ratio range and the flow computer was re-programmed by a trained technician, with the relevant calibration data.

Reference to the customer’s orifice plate data, indicated the adjustable cone meter showed a difference of approximately +/- 4% in the flow rate, over the 3 hour test period (see Fig. 13 and 14). Existing pipework was used to keep costs as low as possible for the trial, no provision was made to include an RTD in the set-up. A fixed value for temperature was therefore entered into the flow computer, which could be corrected as required. Figures 13. and 14. reflect this temperature corrected data.

Each major fluctuation in the diagram indicates an orifice plate change out and/or a separator level adjustment. The customer's operations log showed there were five plate change-outs during this first flow period. Each plate change-out required an experienced operator to then manually adjust the separator pressure, or level, in order to stabilise the flow rate.

The average differential pressure at the adjustable cone meter during this period was 21 inches H20. This was well within the calibrated range of the 100 PSIA and 30” H2O multi-variable transmitter, used with the flow computer. The average flowing pressure was only 1.99 psi, so was very near to the low end of the flowing pressure range. In addition, most of the line pressure was dropped as the gas passed over the cone, so results were significantly affected.

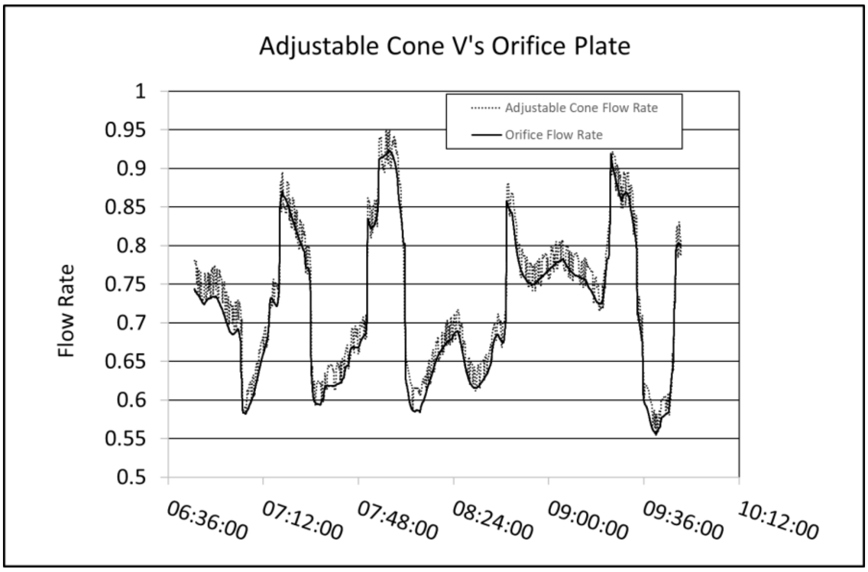

Fig. 13 Adjustable Cone (0.5 β Ratio) and Orifice Flow Rate over 3 Hours

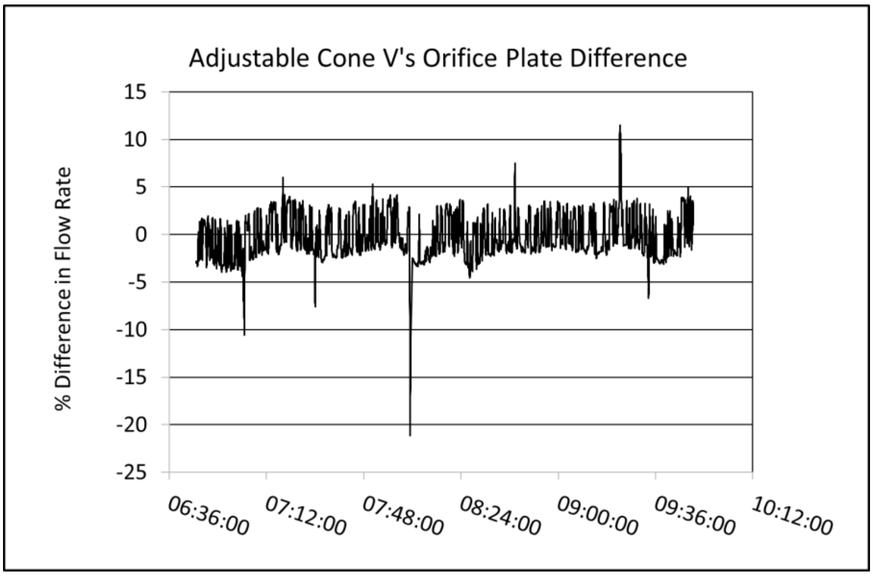

Fig. 14 Precentage Difference between Adjustable Cone (0.5 β Ratio) and Orifice Flow Rate

During a second flow period, the flow rate was only approximately half that experienced during the first flow period. The flowing pressure was barely detectable, at approximately 0.3 psi. As a result, no reliable data was gathered for this period.

2.4.2 Field Test 1 Conclusions

The meter performed as required physically and a sleeve adjustment was successfully conducted at the start of the test. During the test period 5 orifice plate changes were undertaken. The first flowing period provided satisfactory adjustable meter flow data results, which agreed with the orifice plate meter to within +/- 4.% The flowline pressure during the second flowing period was below the calibrated range of the pressure transducer, flowrate analysis was inconclusive. A field technician was trained on the use of the single-run flow computer, changing the calibration data for rnage changes as required. Regular gas sampling took place during the job and new gas SG figures were updated to the flow computer as they were received.

2.4.3 Field Test 2

In order to try to get better quality data, an in-line restriction, consisiting of a section of smaller (2”) diameter pipe, was placed into the line, to try to raise the operating pressure to a recordable level. In practice this did not significantly raise the flowing pressure, which was consistently below 5 psi during the entire flowing period. The meter was placed in high range, in anticipation of a higher flow rate and therefore differential pressure than during the first test, preventing possible over-ranging of the transmitter.

The same technician from the first test, was also in attendance on site, but was unexpectedly crew-changed before flow was initiated. This resulted in the adjustable flow meter being left in the high range. Although it had all the correct calibration data applied, no updates could be made to the gas SG during the test. These had to be corrected for, using the same temperature corrections as used in field test 1.

Results were gathered during the flow period and are presented below in Fig.15 and Fig 16. After correction for temperature and gas SG, the adjustable cone meter read on average 2-5% above the orifice plate meter flow rate readings. These figures broadly agreed with those from the first well, although the flowing pressure was still very low, with an average over the test period of 4.1 psi and an average differential pressure of only 2.99 inches. The same 100 PSIA and 30” H2O multivariable transmiter was used for both tests.

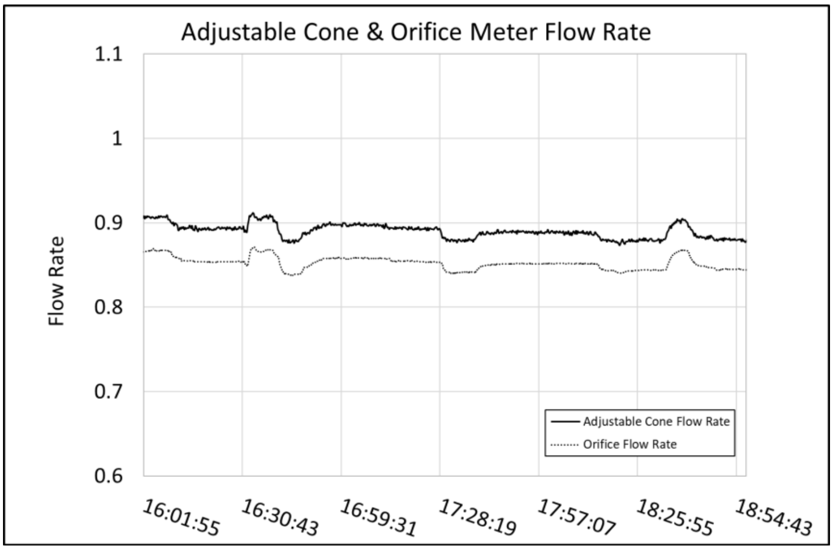

Fig. 15 Adjustable Cone (0.75 β) and Orifice Reading over 3 Hours

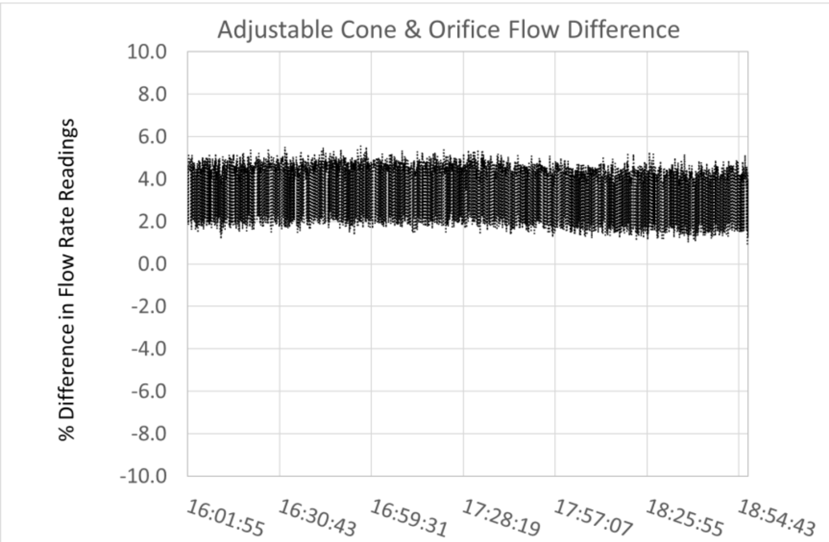

Fig. 16 % Difference between Adjustable Cone (0.75 β Ratio) and Orifice Flow Rate

2.4.4 Field Test 2 Conclusions

The meter performed as required physically in both tests and a sleeve adjustment was successfully conducted prior to the start of test 2. During the test period shown, no orifice plate changes were carried out, so that smooth data could be compared without complications. The flowing period provided satisfactory flow data results which agreed with the orifice plate to within +2-5%.

In all cases the flowing pressure and/or differential pressures were extremely low, so future applications would not be allowed for such flowing conditions. It was suspected that wet gas was present in the flow line, which may have been partly or wholly responsible for the over-reading observed with the adjustable meter.

The orifice plate readings were taken at approximately 290 psi, so any wet gas would be magnified at the cone meter, by comparing the Lockhart-Martinelli (Eq. 8) parameter at the two conditions.

Reliance on a field technician to make the range change, then update the flow computer data would have to be excluded from further jobs, to ensure that the integrity of the results would always be guaranteed. The use of a dual-run flow computer with ability to make changes to the sleeve position and undertake the relevant calculations, would negate the requirement for a technician.

3 FLOW LOOP CALIBRATION & TESTING OF THE 4" 0.45 AND 0.7 Β RATIO METER

3.1 Overview

The flow loop testing was undertaken at NEL Flow Laboratory, East Kilbride, UK.

The 4" meter with adjustable 0.45 & 0.7 β ratio, which was tested included a dual-stream, close-coupled flow computer to overcome reliance on a field technician to make programming changes. The flow computer monitored the flow rate, making automatic adjustment to the flow range as required, by controlling the movement of the sliding sleeve.

If the DP or flowing velocity exceded alarm limits set within the flow computer, a sleeve change logic sub-routine was implemented to adjust the sleeve position. Safety logic functionality included de-activation of the flow calculations during periods of sleeve movement. Alarms would have warned if air pressure failed, or the sleeve failed to travel the specified distance within a specific time.

Exact positioning of the sleeve was achieved via external magnetic sensors, which monitored the position of magnets embedded within the sleeve body. Position data was processed by the flow computer which interacted with electro-pneumatic switches to control the supply of pressurised air to the air motor, switching off the air supply, as the magnet passed under the detector switch.

When the high range magnetic sensor was active, the flow computer used flow calculations and calibration data for the 0.7 β ratio position. When the low range sensor was active, the flow computer used flow calculations and calibration data for the 0.45 β ratio position.

Various designs have been developed to indicate the position of the sliding sleeve. For 4" meter tested, the sliding sleeve's position was verified by an external mechanical pointer, as shown in Fig. 9. Tests were carried out to show the effect of slight variations in the sleeve position upon the differential pressure, at selected flow rates.

The flow computer used differential pressure, flowing pressure, flowing temperature inputs and dry gas calibration data to compute the gas density (ρ_{gas}), compressibility (Z), expansibilty (ε), mass flow rate Q_m and volume flow rate (Q_v) according to the applicable gas measurement standards.

3.2 Test Method

Low - 10 bar(g) and high pressure - 61 bar(g) dry gas calibration was undertaken with the sliding sleeve in both the meter 'low' (0.45 β ratio) and 'high' (0.7 β ratio) operating flow ranges. A representation of the flow loop is shown in Fig 17. Dry nitrogen gas was used as the test medium, being pumped at various rates from minimum to maximum capability of either the flow loop or the meter, whichever was the limiting factor. Tests were conducted in the order shown in Table 2.

Table 2 – Dry Nitrogen Calibration Data

β Ratio	Pressure Bar(g)	Min Δp (mBar)	Max Δp (mBar)	Min q_m	Max q_m
0.45	10	24	500	0.22[2]	1.01
0.7	10	24	850[1]	0.86	4.96
0.7	61	24	850[1]	2.04	12.00[2]
0.45	61	24	500	0.52	2.41

[1] Field use would limit the differential pressure limit to 500 mBar.
[2] Limits of the test facility.

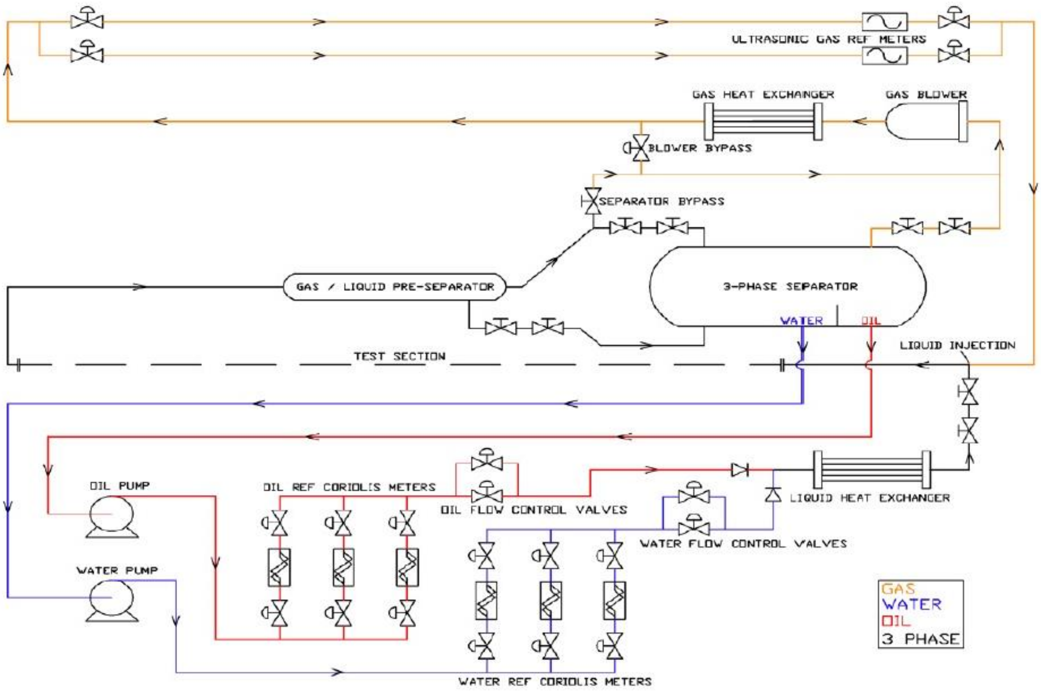

Fig. 17 : Schematic Representation of NEL's High Pressure Wet Gas Facility

The meter was installed in the test line with approximately 10D of 4" pipe upstream and 10D of 4" pipe downstream. A temperature probe was installed downstream of the cone meter. An additional differential pressure transmitter was installed between the upstream pressure tapping and downstream of the temperature transmitter, to measure the overall pressure loss of the meter.

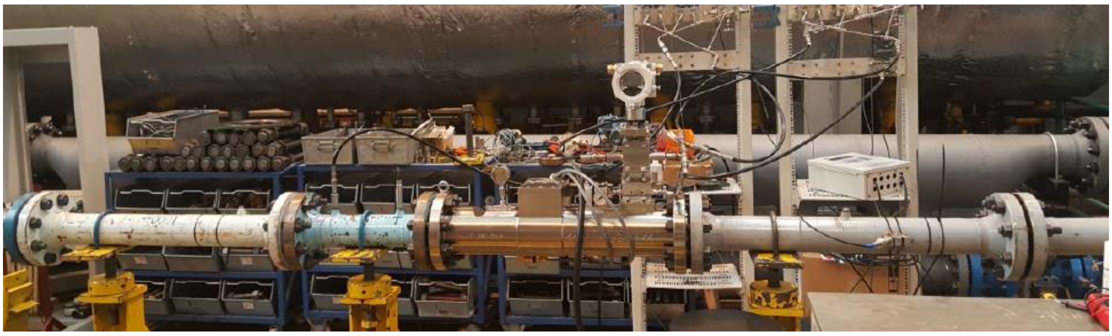

Fig. 18 – 4” Adjustable Cone Flow Meter During Calibration/Testing at NEL

The meter was dry gas calibrated and a series of coefficients of discharge and corresponding Reynolds numbers were obtained using equation (7). These results are shown in Section 3.3.

$$C = \frac{m\sqrt{1-\beta^4}}{\epsilon A_a\sqrt{2\rho_1\Delta p}} \quad (7)$$

Upon completion of the dry gas calibration the meter was wet-gas tested using nitrogen and kerosene substitute Exxsol D80, with a density of 796.1 Kg/m3 at the operating temperature of the facility. The same dry-gas volumentric flow rate range was replicated and D80 was injected at the mixing point, to give a series of wet-gas results. This data was compiled for a Lockhart-Martinelli parameter ranging from 0 to 0.25 and a gas Froude number ranging from of 0.4 to 5.2. These parameters were caulcuated using equations (8) and (9) from chapter 11 of Reader-Harris [3] and NEL [6]. In additon, the pressure loss ratio was calculated using equation (10) from ISO-5167 part 2 [1].

$$\boldsymbol{X} = \left(\frac{\boldsymbol{q_{m,liquid}}}{\boldsymbol{q_{m,gas}}}\right)\sqrt{\frac{\boldsymbol{\rho_{1,gas}}}{\boldsymbol{\rho_{liquid}}}} \quad (8)$$

$$Fr_{gas} = \frac{4q_{m,gas}}{\rho_{1,gas}\pi D^2\sqrt{gD}}\sqrt{\frac{\rho_{1,gas}}{\rho_{liquid}-\rho_{1,gas}}} \quad (9)$$

$$Pressure\ Loss\ Ratio = \frac{\Delta\bar{\omega}}{\Delta p} \quad (10)$$

The cone meter wet gas over-reading is the ratio between the apparent gas mass flow rate ($m_{apparent}$) and the actual gas mass flow (*m*)*.* It was obtained from the reference gas flow meters and is calcluated using equation (11) [6]

$$\emptyset = \frac{\boldsymbol{m_{apparent}}}{\boldsymbol{m}} \quad (11)$$

The apparent gas mass flow rate is given by equation (12)

$$m_{apparent} = \frac{\bar{C}\epsilon A_a\sqrt{2\rho_1\Delta p_1}}{4\sqrt{1-\beta^4}} \quad (12)$$

(see parameter definition list in section 5)

3.3 Dry Gas Test Results

Dry nitrogen gas calibration data is shown in Tables 3, 4, 5 and 6. Combining Tables 3 and 5, gives Fig. 19. Combining Tables 4 and 6, gives Fig. 20 A best-fit line drawn through all the data in each graph allowed a 10 point, evenly spaced Reynolds Number v's Discharge Coefficient table to be produced. For each β ratio this data would be programmed into the flow computer, for subsequent field trials.

Table 3 – NEL Test Point, Reynolds Number, Discharge Coefficient and Total Uncertainty for the 0.7 β Ratio Range at 10 Bar(g).

Test Point	Pipe Reynolds Number (-)	Discharge Coefficient (-)	U_{tot} %
T6661-s01-3	6.3533E+05	0.8212	0.477
T6661-s01-4	6.3576E+05	0.8215	0.477
T6661-s01-5	6.3571E+05	0.8216	0.477
T6661-s01-6	3.6625E+06	0.8265	0.672
T6661-s01-7	3.6580E+06	0.8257	0.672
T6661-s01-8	3.6584E+06	0.8258	0.671
T6661-s01-9	2.7066E+06	0.8247	0.498
T6661-s01-10	2.7060E+06	0.8249	0.498
T6661-s01-11	2.7063E+06	0.8249	0.498
T6661-s01-12	3.6548E+06	0.8258	0.668
T6661-s01-13	1.7083E+06	0.8241	0.431
T6661-s01-14	1.7075E+06	0.8238	0.431
T6661-s01-15	1.7077E+06	0.8241	0.431
T6661-s01-16	9.1764E+05	0.8239	0.478
T6661-s01-17	9.1653E+05	0.8234	0.478
T6661-s01-18	9.1646E+05	0.8238	0.478
T6661-s01-19	9.1505E+05	0.8233	0.478
T6661-s02-20	9.1600E+05	0.8229	0.477

Table 4 – NEL Test Point, Reynolds Number, Discharge Coefficient and Total Uncertainty for the 0.45 β Range at 10 Bar(g).

Test Point	Pipe Reynolds Number (-)	Discharge Coefficient (-)	U_{tot} %
T6661-s02-2	2.0546E+05	0.9031	0.479
T6661-s02-3	2.0522E+05	0.9038	0.479
T6661-s02-4	2.0532E+05	0.9038	0.479
T6661-s02-5	9.3258E+05	0.9098	0.514
T6661-s02-6	9.3302E+05	0.9096	0.514
T6661-s02-7	9.3297E+05	0.9095	0.513
T6661-s02-8	6.6119E+05	0.9068	0.444
T6661-s02-9	6.6139E+05	0.9070	0.444
T6661-s02-10	6.6130E+05	0.9072	0.444
T6661-s02-11	4.1837E+05	0.9035	0.423
T6661-s02-12	4.1813E+05	0.9029	0.423
T6661-s02-13	4.1800E+05	0.9032	0.423
T6661-s02-14	2.9492E+05	0.9037	0.479
T6661-s02-15	2.9441E+05	0.9029	0.479
T6661-s02-16	2.9432E+05	0.9027	0.479
T6661-s02-17	2.9407E+05	0.9032	0.479
T6661-s02-18	2.0455E+05	0.9033	0.479
T6661-s02-19	2.0480E+05	0.9038	0.479

Table 5 – NEL Test Point, Reynolds Number, Discharge Coefficient and Total Uncertainty for the 0.7 β Ratio Range at 62 Bar(g).

Test Point	Pipe Reynolds Number (-)	Discharge Coefficient (-)	U_{tot} %
T6661-s04-2	1.4278E+06	0.8256	0.476
T6661-s04-3	1.4298E+06	0.8257	0.476
T6661-s04-4	1.4292E+06	0.8259	0.476
T6661-s04-5	1.4288E+06	0.8257	0.476
T6661-s04-6	8.3982E+06	0.8276	0.427
T6661-s04-7	8.3945E+06	0.8273	0.427
T6661-s04-8	8.3958E+06	0.8276	0.427
T6661-s04-9	6.1058E+06	0.8263	0.421
T6661-s04-10	6.1050E+06	0.8265	0.421
T6661-s04-11	6.1032E+06	0.8266	0.421
T6661-s04-12	3.8049E+06	0.8247	0.418
T6661-s04-13	3.8061E+06	0.8247	0.418
T6661-s04-14	3.8051E+06	0.8244	0.418
T6661-s04-15	2.0392E+06	0.8260	0.479
T6661-s04-16	2.0397E+06	0.8259	0.479
T6661-s04-17	2.0408E+06	0.8262	0.479
T6661-s04-18	2.0417E+06	0.8269	0.479

Table 6 – NEL Test Point, Reynolds Number, Discharge Coefficient and Total Uncertainty for the 0.45 β Ratio Range at 62 Bar(g).

Test Point	Pipe Reynolds Number (-)	Discharge Coefficient (-)	U_{tot} %
T6661-s03-2	4.5662E+05	0.9019	0.479
T6661-s03-3	4.5815E+05	0.9028	0.479
T6661-s03-4	4.5827E+05	0.9031	0.479
T6661-s03-5	4.5798E+05	0.9024	0.479
T6661-s03-6	2.1137E+06	0.9187	0.421
T6661-s03-7	2.1143E+06	0.9186	0.421
T6661-s03-8	2.1140E+06	0.9190	0.421
T6661-s03-9	1.4893E+06	0.9144	0.418
T6661-s03-10	1.4894E+06	0.9143	0.418
T6661-s03-11	1.4892E+06	0.9143	0.418
T6661-s03-12	9.3758E+05	0.9101	0.419
T6661-s03-13	9.3688E+05	0.9095	0.419
T6661-s03-14	9.3630E+05	0.9100	0.477
T6661-s03-15	6.6598E+05	0.9071	0.477
T6661-s03-16	6.6640E+05	0.9073	0.477
T6661-s03-17	6.6561E+05	0.9078	0.477
T6661-s03-18	6.6600E+05	0.9076	0.477

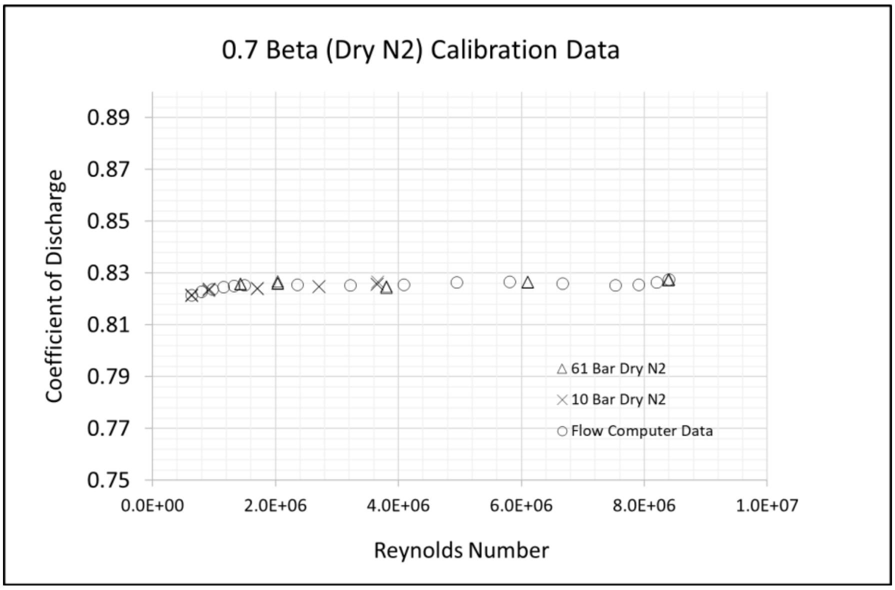

Fig. 19 0.7 β Ratio Dry N2 Calibration Data at 10 and 62 Bar(g)

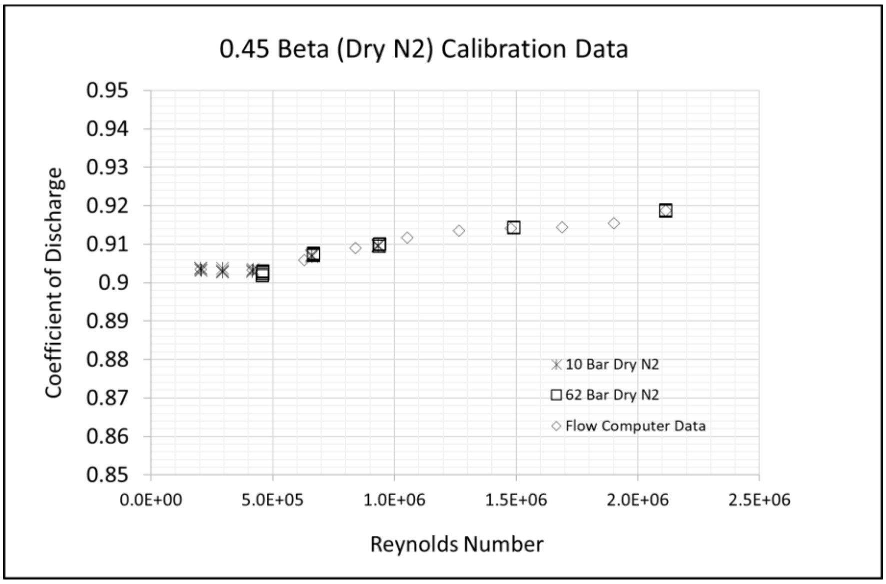

Fig. 20 0.45 β Ratio Dry N2 Calibration Data at 10 and 62 Bar(g)

Turndown ratio of the adjustable cone meter is demonstrated in table 7 and 8. An overall turndown ratio, of the calibrated range is 54.5:1 by mass flow rate and 51.4 :1 by volume flow rate. By Reynolds number, the turndown ratio is 41:1 from tables 3 to 6. An example of the flow range of the meter under field conditions using a 100 Barg, 500 mBar multi-variable transmitter is shown in Fig. 21. Calibration points are over-drawn for clarity.

Table 7 – Mass Flow Rates and Calibrated Turndown Ratio

β Ratio	Pressure Bar(g)	Min q_m (Kg/sec)	Max q_m (Kg/sec)	Turndown Ratio	Calibrated Turndown Ratio
0.45	10	0.22[2]	1.01	4.6	54.5[3]
0.45	61	0.52	2.41	4.6	
0.7	10	0.86	4.96	5.8	
0.7	61	2.04	12.00[2]	5.9	

[2] Limits of the test facility.
[3] Calibrated turndown = q_m max at 61 Bar(g) divided by q_m min at 10 Bar(g)

Table 8 – Volumetric Flow Rates and Calibrated Turndown Ratio

β Ratio	Pressure Bar(g)	Min q_v (m3/Hr)	Max q_v (m3/Hr)	Turndown Ratio	Calibrated Turndown Ratio
0.45	10	61.09	272.67	4.5	51.4[4]
0.45	61	26.2	120.5	4.6	
0.7	10	235.15	1345.63	5.7	
0.7	61	102.26	600.91	5.9	

[4] Calibrated turndown = q_v max at 61 Bar(g) divided by q_v min at 10 Bar(g)

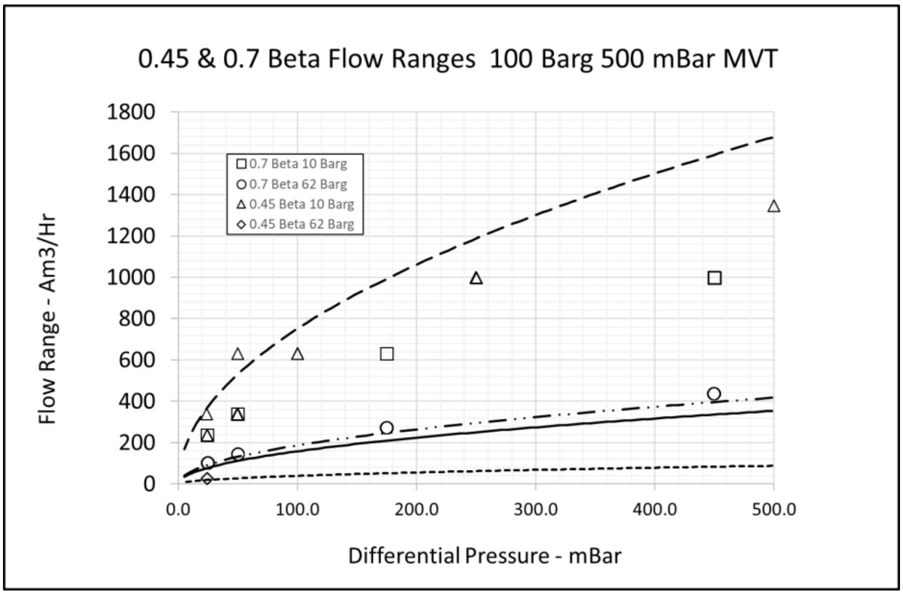

Fig. 21 N2 Calibration Data Overlaid on 100 Bar(g) 500 mBar MVT Range Graph

3.3.1 Sleeve Adjustment & DP Settle-back Time

The time taken for the sleeve to fully adjust from the high to low and from the low to high operating ranges, was assessed at 10 and 62 Bar(g). The time taken for the differential pressure to settle back to pre-sleeve adjustment conditions was also assessed. Fig 22 shows 1 switching operation from low (500 mBar) to high (270 mBar) and back to low again. The sleeve took on average 15 seconds to switch in either direction at both pressures. The differential pressure settle-back time was approximately 10-12 seconds, after sleeve movement was complete.

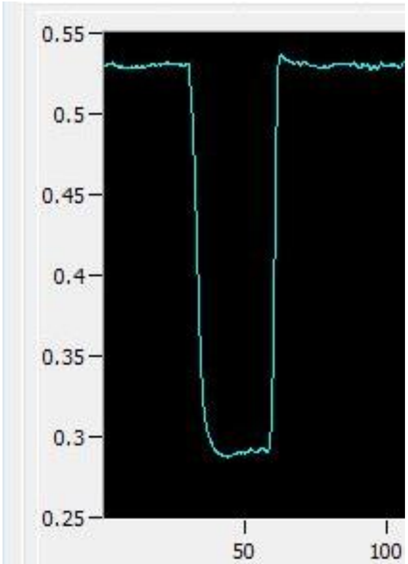

Fig. 22 – Sleeve Adjustment & DP Settle-back Time

During each switching operation the flow computer was locked, to stop logging the flow rate. Alternatively, the flow computer can also be set to record data using the last known values, depending on the user’s choice.

3.3.2 Sleeve Positioning

In order to assess the accuracy of the sleeve positioning, a test was undertaken where the sleeve was deliberately over and under displaced from its optimum design position relative to the position of the cone.

In the optimum design position, the sleeve fully covers the cone at its largest diameter ($Ød_c$). In the under-displaced position, the sleeve may not fully cover the cone at its largest diameter ($Ød_c$). In the over-displaced position, the cone is positioned further within sleeve than the optimum position.

An over displacement of 7% produced no discernable effect on differential pressure, while 7% under-displacement produced an increase in the differential pressure of 0.29%.

This slight increase in the DP at the under-displacement position, could relate to increased turbulence as the gas travels from the relatively large meter bore, into the throat between the sleeve and the cone. Future tests will be carried out to further characterise this effect.

3.3 Wet Gas Test Results

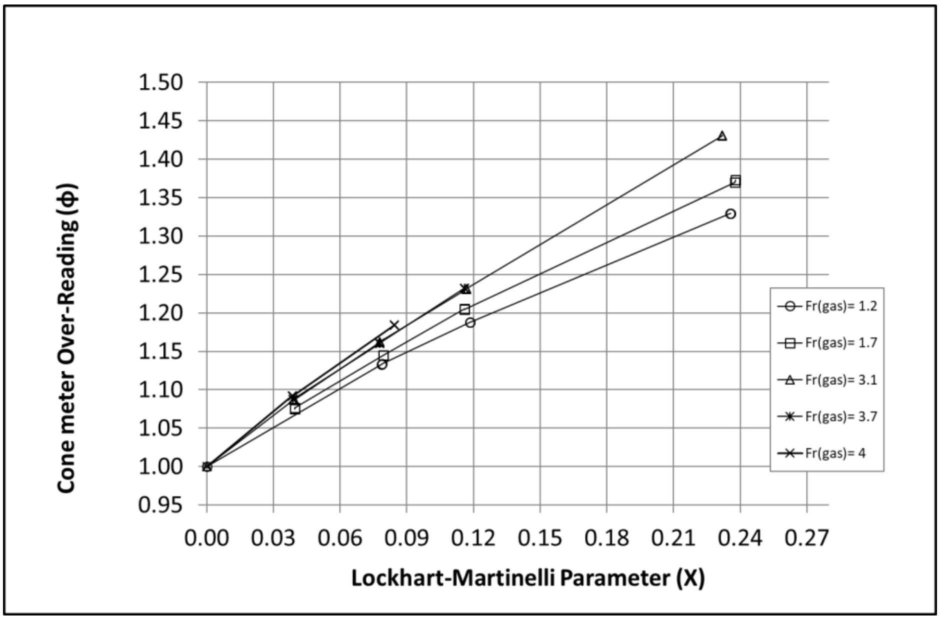

Fig. 23 Wet Gas Calibration Data 0.7 β Ratio 10 Bar(g) $\rho_{1\ gas}/\rho_{\ liquid}$ = 0.016

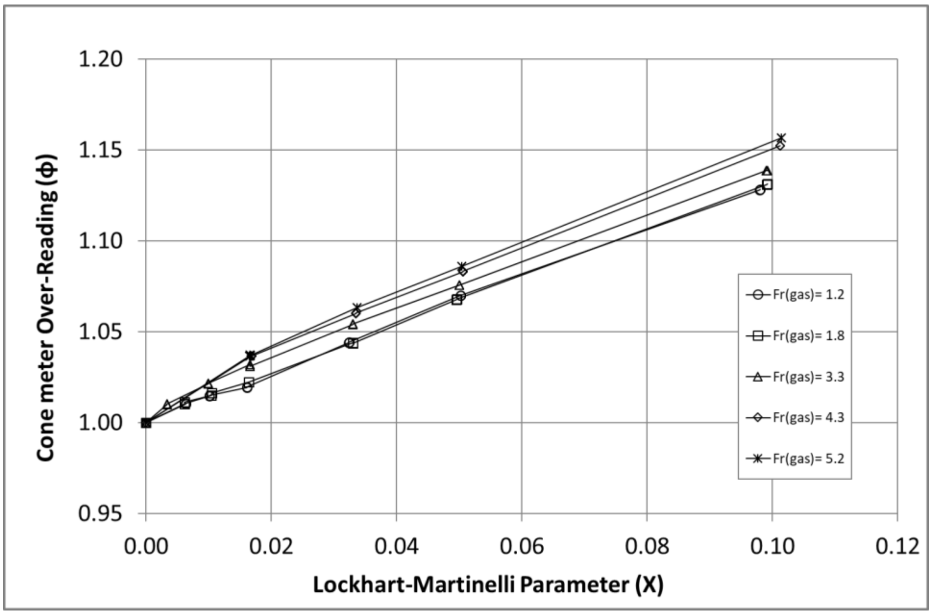

Fig. 24 Wet Gas Calibration Data 0.7 β Ratio 62 Bar(g) $\rho_{1\ gas}/\rho_{\ liquid}$ = 0.009

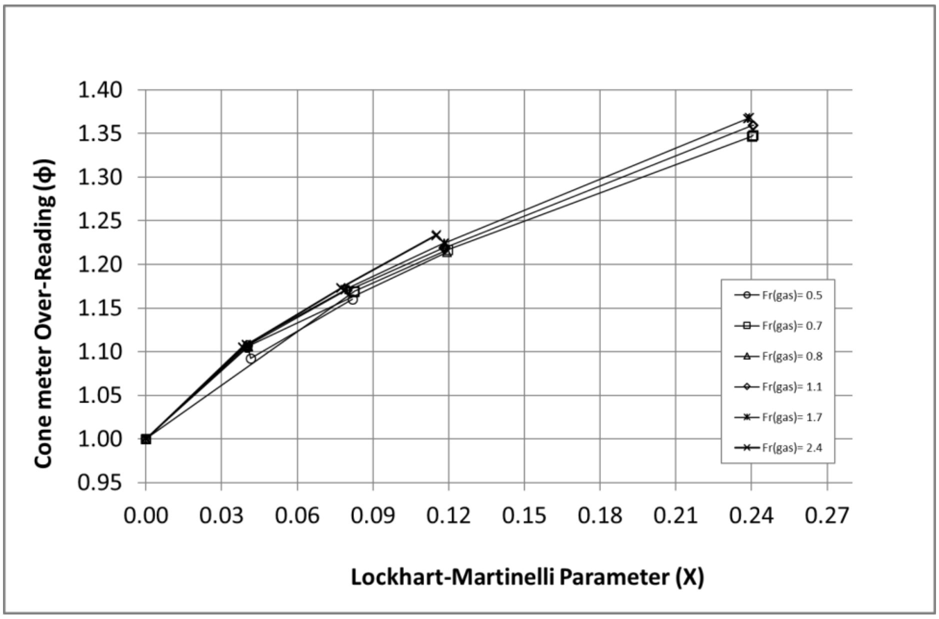

Fig. 25 Wet Gas Calibration Data 0.45 β Ratio 10 Bar(g) $\rho_{1\ gas}/\rho_{\ liquid}$ = 0.016

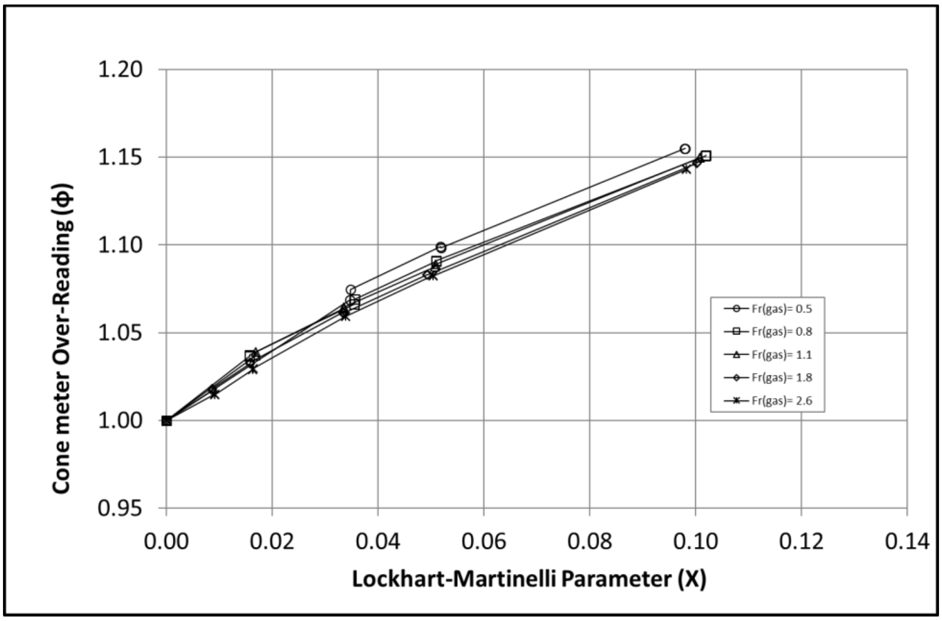

Fig. 26 Wet Gas Calibration Data 0.45 β Ratio 62 Bar(g) $\rho_{1\ gas}/\rho_{\ liquid}$ = 0.009

Although recorded, pressure loss ratios, are not presented in this paper, due to time constraints in processing and examining the data.

3.4 Analysis

3.4.1 Dry Gas

Data for the 0.7 β ratio showed that an average uncertainty of 0.49% applies over the calibrated operating range. The average repeatability of points over the same range is +/- 0.02%.

The reproducibility of data which could be expected when the meter is switched from high to low operating range, then immediately switched back to high again, is 0.25%. Point T6661-s0-20 in Table 3 is an example of a reproducibility test.

Data for the 0.45 β ratio showed that an average uncertainty of 0.457% applies over the calibrated operating range. The average repeatability of points over the same range is +/- 0.03%.

3.4.2 Wet Gas

Over-reading (ϕ) was plotted as a functon of the Lockhart-Martinelli parameter (X) and Gas Froude Number (Fr_g) for 0.45 and 0.7 B at 10 and 62 Bar(g). The results are shown in Fig. 22- 26.

The amount of over-reading reduced as pressure increased. This is as expected, since higher pressures cause a reduction in X. For both β ratios at 10 bar(g), the maximum over-reading was consistent at 1.35, when X = 0.24. For both β ratios at 62 bar(g), the maximum over-reading was consistent at 1.15, when X = 0.1.

The plotted curves were straight line in nature, for the 0.7 β ratio range. In the 0.45 β ratio range the slope of the curve increased as X neared zero, as observed by Reader-Harris[3]. Studies to investigate the reason for this will be part of future work.

Comparisons can be drawn to Reader-Harris' and Steven's venturi data [3,7,8] (in Fig. 27). It appears that the adjustable cone meter over-reading is less affected by wet gas than a venturi meter is, in either β ratio.

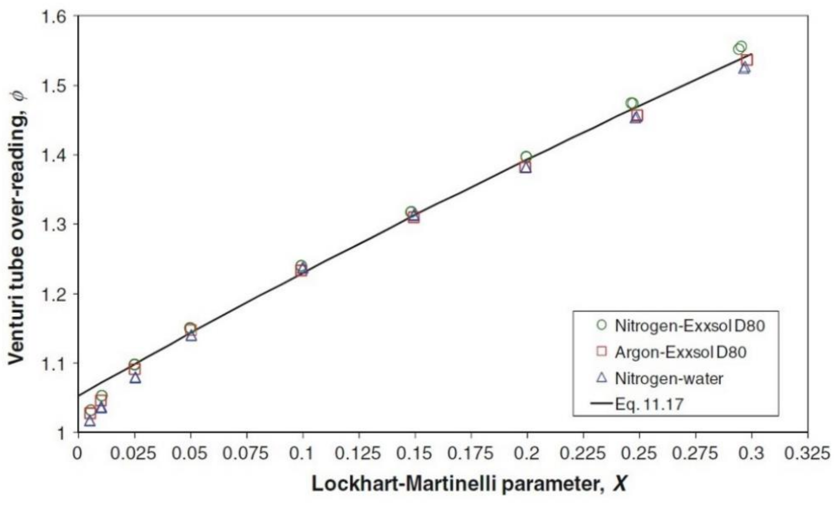

Fig. 27 NEL over-reading data for Fr_{gas} = 1.5 β = 0.6 $\rho_{1\,gas}/\rho_{liquid}$ = 0.024

4 CONCLUSIONS & FURTHER DEVELOPMENTS

An adjustable cone meter provides excellent turndown ratio when used to measure dry gas. Turndown ratios in excess of 50:1 were easily demonstrated by the test results shown.

Actual turndown ratios achieved in field use will depend on the transmitter device(s) used. A user could expect turndown ratios as much as 100:1 or 200:1, with increased uncertainty.

Automatic switching of the cone β ratio range through accurate and reliable movement of the internal sliding sleeve, was proven. This negates the requirement for a technician to monitor and switch orifice plates during field operations.

Use of a dual-stream flow computer programmed with both sets of dry gas calibration results, was proven. This further negates the requirement for a technician to re-programme a single-stream flow computer after each sliding sleeve movement.

The meter tested showed excellent uncertainty (< 0.5%), repeatability (+/- 0.02%) and reproducibility (0.25%) under test conditons.

Extremely acurate sleeve positioning is not required. A 7% over shoot of the sleeve total movement does not affect the reading, but an undershoot caused the differential pressure to rise by 0.29%.

Testing and analysis undertaken to date indicates that an adjustable cone meter will over-read less than a venturi in wet gas conditions. The use of a single average discharge coeffient in equation 12 is questioned, since cone meters have a varying discharge coefficient relating to the Reynolds number. Any effect of varying C with Reynolds number will be further investigated in future test work and by futher analysis of this test data.

No attempt was made at this stage to make any correction for over-read in wet gas conditions. The tests conducted in this study represent initail investigation into the magintude of the effect, at different ranges of X and Fr_{gas} number. Further understanding of the pressure loss ratio and if/how it maybe used to detect low values of X is required.

4.1 Further Design Development

Further analysis is required to fully understand the wet gas effect on an adjustable cone meter. We wish to extend our understanding of how the meter performs: like an orifice, a venturi, a standard cone meter, or does one β operating range or size perform differently to another?

Finite Element Analyses and Computational Fluid Dynamics (CFD), will enhance our understanding of the mechanical, hydraulic and physical aspects of building larger meter sizes. Is it possible, and what is invloved, to build (say) an 18″ or 24″ version?

Investigation by CFD will provide insights as to the expected outcomes of these studies. Small and exact changes in internal geometries, flowing conditions and surface finishes, can lead to an early understanding if a particular design change may or may not be successful.

Based on test findings, CFD modelling will be utilised to further characterise an adjustable cone meter's performance across a wide range of β ratios. Varying densities of liquids can be used in wet gas studies, so it maybe possible to better predict the likely performance of gas/oil or gas/water mixtures and to design more effective physical test plans.

CFD will assist in understanding how higher pressures >100 bar(g) (1440 psi) and/or temperatures >100 Deg C (212 Deg F), which cannot be easily laboratory tested, will affect the adjustable cone meter's performance.

Various adjustable meter design development opportunities are being investigated, including the application of advanced materials and manufacturing techniques, and the application of artificial intelligence and machine learning software. Real-time remote access and control, down-hole and sub-sea applications are being investigated.

5 NOTATION

$ØD_m$ = Adjustable Cone Meter Inside Diameter, (m)
$ØD_s$ = Adjustable Cone Meter Sleeve Inside Diameter, (m)
ØD or D = Standard Cone Meter Inside Diameter, (m)
$Ød_c$ = Cone Outside Diameter, (m)
β_{low} = Adjustable Cone Meter Low Range Beta Ratio
β_{high} = Adjustable Cone Meter High Range Beta Ratio
q_m or m = Gas Mass Flow Rate (Kg/sec)
C or Cd = Coefficent of Discharge or Discharge Coefficient (no units)
$\bar{C}$ or $\bar{Cd}$ = Coefficent of Discharge, due to over-reading (no units)
ε = Expansibility or expansion factor (no units)
π = 3.14159
Δp = Differential Pressure of the flowing fluid/gas (Pa)
ρ_1 = Flowing density of the fluid/gas (Kg/m3)
p_1 =Upstream pressure (Pa)
k = Isentropic Exponent, also known as Specific Heat Ratio and C_p/C_v
A_a = Cross Sectional Area, between the cone and the sleeve/meter ID (m^2)
X =Lockhart-Martinelli parameter (no units)
g = acceleartion due to gravity, 8.80665 m/s^2
Fr_{gas} = Gas Froude Number (no units)
ϖ = Pressure Loss or overall pressure loss of the meter (Pa)
Ø = gas over-reading (no units)
$m_{apparent}$ = The apparent gas flow rate
Z = Gas compressibility

6 REFERENCES

[1] ISO 5167-2: Measurement of Fluid Flow by means of Pressure Differential Devices Inserted in Circular Cross-Section Conduits Running Full – Part 2 Orifice Plates, 2003

[2] ISO 5167-5: Measurement of Fluid Flow by means of Pressure Differential Devices Inserted in Circular Cross-Section Conduits Running Full – Part 5 Cone Meters, 2016

[3] M. Reader-Harris, "Orifice Plates and Venturi Tubes", ISBN 978-3-319-16880-7, 2015.

[4] M. Reader-Harris, E. Graham, "An Improved Model for Venturi-tube Over Reading in Wet Gas", 27th International North Sea Flow Measurement Workshop, Paper 7, 2009.

[5] D.G. Stewart, M. Reader-Harris, R.J.W Peters, "Derivation Of An Expansibility Factor For The V-Cone Meter", Flow Measurement 2001 – International Conference.

[6] E. Graham "NEL Certificate of Calibration – 2018-586 & 2015-679".

[7] D.G. Stewart, D. Hodges, R.N. Steven, R J W Peters, "Wet Gas Metering with V-Cone Meters", 20th North Sea Flow Measurement Workshop October 2002, Perthshire, UK.

[8] R.N. Steven, "Wet Gas Metering with a Horizontally Mounted Venturi Meter", Journal of Flow Measurement and Instrumentation 12 (2002) 361-372